

Preparation and characterisation of exfoliated muscovite/poly(2,3-dimethylaniline) nanocomposites with an enhanced anticorrosive performance

Shanhua Chen¹ ✉, Fang Chen¹, Yuli Di^{1,2}, Shihu Han¹, Xiaodong Zhu^{1,3}

¹College of Materials and Chemistry & Chemical Engineering, Chengdu University of Technology, Chengdu 610059, People's Republic of China

²School of Science, Xichang University, Xichang 615000, People's Republic of China

³College of Mechanical Engineering, Chengdu University, Chengdu 610106, People's Republic of China

✉ E-mail: chensh@cdu.edu.cn

Published in Micro & Nano Letters; Received on 26th January 2020; Revised on 9th March 2020; Accepted on 15th April 2020

The application of organic muscovite (OM)/Poly(2,3-dimethylaniline) (OM/P(2,3-DMA)) nanocomposites in corrosion protection is proposed in this Letter. The OM/P(2,3-DMA) nanocomposites were successfully prepared by in situ chemical oxidation polymerisation of poly(2,3-dimethylaniline). The OM/P(2,3-DMA) coating considerably improved the anticorrosion performance of steel. Compared to the P(2,3-DMA) coating, the OM/P(2,3-DMA) with loading of 6 wt% of OM displayed an optimal anticorrosive performance.

1. Introduction: Metal corrosion is a major global problem. Metals can be protected from corrosion using several methods. The application of organic coatings is the most common and convenient method to ensure the efficient protection of metals from corrosion [1]. Polyaniline is most popular because of its simple synthesis method, good environmental stability, low cost, special optics and magnetism [2, 3]. Poly(2,3-dimethylaniline) [P(2,3-DMA)] is one of the main derivatives of polyaniline, which exhibits considerable solubility and good processability. Thus, it is extensively used in corrosion protection, paints, catalysis and dyestuff [4]. Yin *et al.* [5] reported that P(2,3-DMA) can be applied to steel sheets due to its good corrosion resistance. Many pigments with a lamellar or plate-like shape have been introduced into polymeric coatings to effectively increase the length of diffusion pathways for oxygen and water as well as to decrease the permeability of the coating [6].

Until now, TiO₂ [7], muscovite [8], halloysite [9] and other inorganic materials have been used as fillers and catalysts [10, 11] to prepare nanocomposites. The polymer/clay nanocomposites (PCNs) are hybrid materials composed of organic polymer matrix and well dispersed inorganic clay composed of silicate sheets [12]. Recently, PCNs with intercalated or exfoliated structures have been successfully proved to enhance the corrosion resistance of the polymers on the metal surfaces [13, 14]. Muscovite has a monoclinic structure with the space group (C2/c) and the following cell parameters $a=5.18$ Å, $b=8.99$ Å, $c=20.07$ Å and $\beta=95.751$ Å. It is a 2 : 1 phyllosilicate silicate mineral with ideal composition of $KAl_2(Si_3AlO_{10}(OH)_2$. Each layer is composed of two tetrahedral sheets and one dioctahedral sheet, sandwiched between two tetrahedral sheets [15]. As the forces perpendicular to cleavage plane (001) are relatively weak, the intercalation of small molecules between the layers parallel to (001) is easy [14]. Microcrystalline muscovite occurred in western Sichuan, China was first discovered by Sichuan Xinju Mining Resources Development Co., Ltd. in 1997. It is a new kind of non-metallic mineral resource with high chemical purity (low content of aluminum content, iron and magnesium), high crystallinity, fine crystalline particles, smooth surface, excellent corona resistance, light colour, large-size deposit and low mining cost [16]. Many studies have investigated the preparation of PCNs using muscovite [8, 15, 16]. As the forces that hold the stacks together are relatively weak, the intercalation of small molecules between the layers is easy [14]. However, there are no reports on the

synthesis, characterisation and corrosion resistance of the muscovite/P(2,3-DMA) nanocomposites. In this Letter, we attempt to modify the compatibility of muscovite and polymers, increase the interplanar spacing of natural muscovite by heat treatment and ion exchange, prepare organic muscovite (OM)/P(2,3-DMA) nanocomposites and evaluate the anticorrosion properties of the OM/P(2,3-DMA) nanocomposites.

2. Experimental: Preparation of OM: muscovite was ground in an agate mortar and heated to 750°C for 5 h at 5°C/min in a temperature-programmed muffle furnace to obtain heat-treated muscovite, and then soaked in 6 M HNO₃ solution for 5 h. Subsequently, the mixture was placed in a constant-temperature water bath under magnetic stirring at 80°C for 5 h. Then, 1 g of muscovite and 10 g of LiNO₃ were thoroughly mixed in an agate mortar and then heated in a muffle furnace for 10 h at 300°C. The product is named as Li-M. Next, 1 g of Li-M was sonicated in distilled water at room temperature for 20 min to ensure homogeneous dispersion of Li-M in water. Then, 1 g of CTAB was added. Finally, the mixture was placed in a constant-temperature water bath and ultrasonically dispersed for 1 h under magnetic stirring at 80°C for 5 h. The obtained CTAB/muscovite composites were named as OM.

Preparation of P(2,3-DMA), pure muscovite/Poly(2,3-dimethylaniline) (PM/P(2,3-DMA)) and OM/P(2,3-DMA) nanocomposites: The samples were prepared by in situ chemical oxidation polymerisation in the presence of H₃PO₄ acting as doped acid. Initially, an appropriate amount of 2,3-DMA was introduced into 50 mL of H₂O under magnetic stirring at room temperature. Next, H₃PO₄ and 2,3-DMA with a molar ratio of 1:2.5 was added to the mixture. Then, water-soluble initiator ammonium persulfate (APS) (at a 2,3-DMA)/APS molar ratio of 1 : 2 was added dropwise to the mixture under vigorous stirring at room temperature, and the reaction was continued for 10 h at 30°C by constant stirring. The precipitated P(2,3-DMA) salt was obtained by filtration. To prepare the PM/P(2,3-DMA) with 4 wt.% of muscovite, and OM/P(2,3-DMA) with 1–8 wt.% of OM, PM or OM was added to P(2,3-DMA) prior to polymerisation. The remaining steps were similar to those in case of preparation of the P(2,3-DMA). Additionally, OM/P(2,3-DMA) with 1, 2, 4, 6 and 8 wt.% of OM were labelled as OM1/P(2,3-DMA), OM2/P(2,3-DMA), OM4/P(2,3-DMA), OM6/P(2,3-DMA) and OM8/P

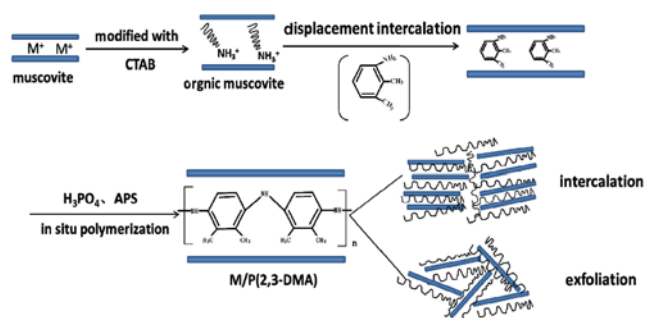


Fig. 1 Preparation process for OM/P(2,3-DMA) nanocomposites

(2,3-DMA), respectively. The preparation of M/P(2,3-DMA) nanocomposites is illustrated in Fig. 1.

Preparation of the coating: P(2,3-DMA) or OM/P(2,3-DMA) was suspended in deionised water and ultrasonically dispersed for 0.5 h. The epoxy resin and epoxy resin curing agent were mixed with the suspension under magnetic stirring. A uniform composite was obtained after vigorous stirring.

The X-ray diffraction (XRD) patterns of muscovite, P(2,3-DMA), PM/P(2,3-DMA) and OM/P(2,3-DMA) were recorded on an Ultima IV diffractometer. The Fourier transform infrared (FTIR) spectrum of the samples was characterised by using the Agilent Cary 630 spectrometer. KBr was used to prepare the samples. The TGA of the samples was investigated using a NETZSCH STA409PC analyser under a nitrogen atmosphere with a heating rate of 10°C/min. The morphological studies of the samples were subjected to scanning using a Quanta 250 FEG scanning electron microscope (SEM) at an accelerating voltage of 20 kV. The corrosion resistance of the P(2,3-DMA) and OM/P(2,3-DMA) coating on a steel sheet was evaluated in a 3.5 wt% saline solution using the CHI660E (CH Instruments, Shanghai, China) electrochemical workstation.

3. Results and discussion: The XRD patterns of muscovite, Li-M and OM are presented in Fig. 2a, in which the low-angle peak of muscovite shifts from $2\theta = 8.73^\circ$ to $2\theta = 6.38^\circ$. By use of Scherrer equation, the calculated interplanar spacing d_{002} of the (002) plane of the pure muscovite, Li-M and organically treated muscovite is 1.05, 1.21 and 1.38 nm, respectively. The organically treated muscovite with effectively expanded interplanar spacing is beneficial for the later intercalation of the 2,3-DMA monomer into muscovite [16, 17]. Fig. 2b showed the XRD pattern of pure muscovite, PM/P(2,3-DMA), OM/P(2,3-DMA) and P(2,3-DMA). The characteristic diffraction peak of muscovite ($2\theta = 6.8^\circ$) was not observed in OM/P(2,3-DMA). The disappearance of the clay 002 peak in the composite can be mainly attributed to the polymerisation of the 2,3-DMA monomer in the muscovite interlayer, resulting in the intercalation and exfoliation of the muscovite layer [18]. For comparison, the PM/P(2,3-DMA) composite was also prepared. It is clear that the muscovite 002 diffraction peak appeared at $2\theta = 6.8^\circ$ of PM/P(2,3-DMA), which indicate that during the formation of PM/P(2,3-DMA), 2,3-DMA is not intercalated between the muscovite layers. The organic treatment of muscovite can be used to effectively improve the properties of the OM/P(2,3-DMA) nanocomposites. Fig. 2c presents the XRD pattern of muscovite, P(2,3-DMA), and OM/P(2,3-DMA) nanocomposites with different content of OM. P(2,3-DMA) does not have a low-angle diffraction peak, indicating that it is an amorphous structure. In case of the OM/P(2,3-DMA) nanocomposites, diffraction peaks cannot be observed at low angles when the content of muscovite is low, which denotes that when 2,3-dimethylaniline is polymerised, the polymer is successfully inserted into the muscovite layer to cause it to peel off or the interval between the layers is too large.

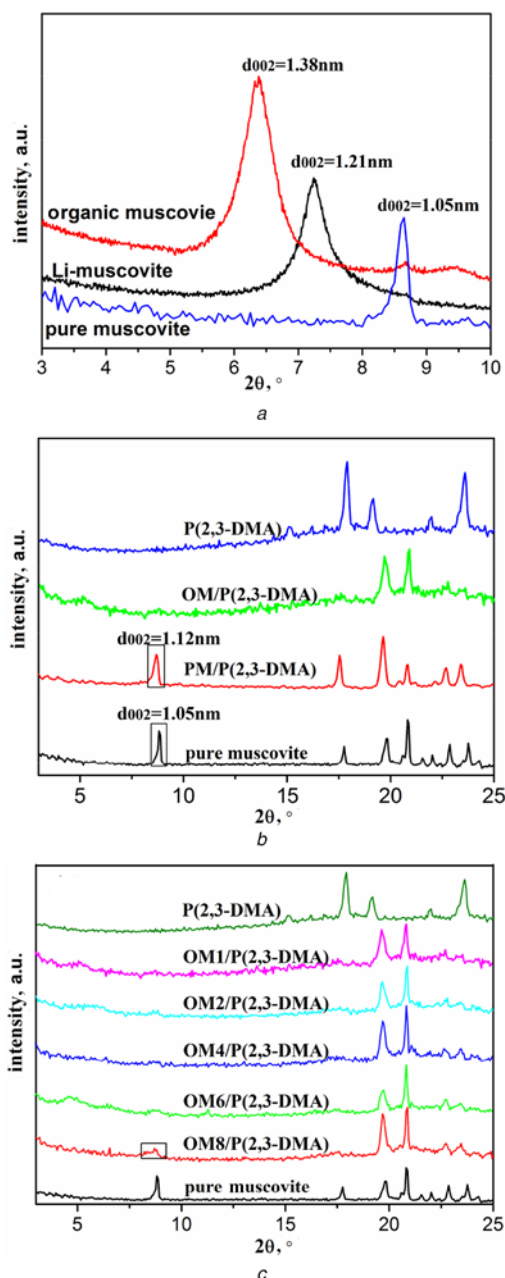


Fig. 2 XRD patterns of
a PM, Li-M, and OM
b PM, PM/P(2,3-DMA), OM/P(2,3-DMA), and P(2,3-DMA)
c PM, P(2,3-DMA), and OM/P(2,3-DMA) with a different M concentrations

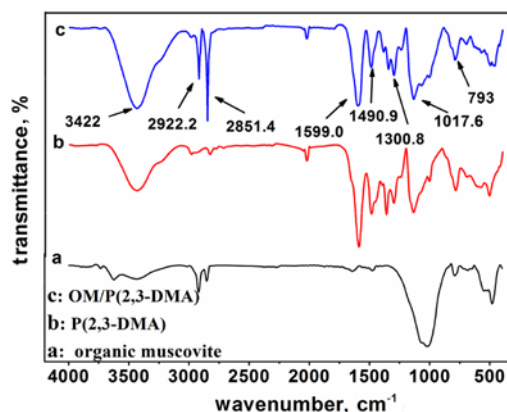


Fig. 3 FTIR spectrum of OM, P(2,3-DMA) and OM/P(2,3-DMA)

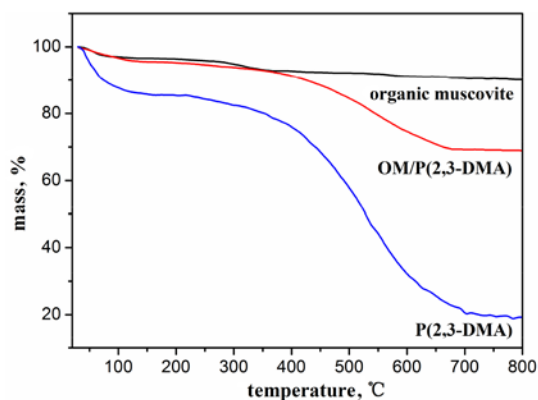


Fig. 4 TGA curves of OM, OM/P(2,3-DMA) and P(2,3-DMA)

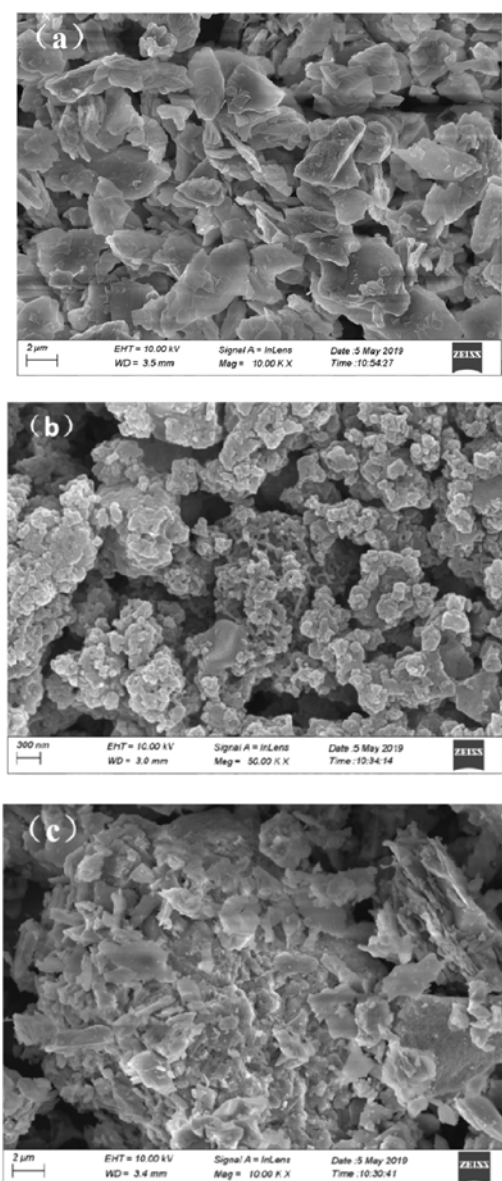


Fig. 5 SEM images of
a PM
b P(2,3-DMA)
c OM/P(2,3-DMA)

However, when the content of muscovite is considerably high (8%), the low-angle peak of the composites can be still observed. Thus, polymer intercalation cannot cause muscovite to peel off or effectively enlarge the layer spacing [19].

The FTIR spectra of the OM, P(2,3-DMA) and OM/P(2,3-DMA) nanocomposites are presented in Fig. 3. For the FTIR spectra of the OM/P(2,3-DMA) nanocomposites, the peak at 1300 and 1599 cm^{-1} can be attributed to the C–N extension of the benzene ring and C=N stretching in the OM/P(2,3-DMA) nanocomposite, respectively. The bands at $\sim 793\text{ cm}^{-1}$ is the OH bending vibrations with respect to the silicate plate in the muscovite structure, whereas the peak at 3422 cm^{-1} is the OH groups between the tetrahedral and octahedral sheets [15]. The main characteristic peaks of P(2,3-DMA) and muscovite were observed in the FTIR spectra, confirming the successful preparation of the OM/P(2,3-DMA) nanocomposites.

The TGA patterns of OM, P(2,3-DMA) and OM/P(2,3-DMA) are shown in Fig. 4. The TGA curves presented three stages. The first stage is mainly the moisture loss occurred at $\sim 91^\circ\text{C}$. The second stage of weightlessness at $\sim 252^\circ\text{C}$ can be attributed to the decomposition of organic modifiers in muscovite. The weight loss takes place near 367°C probably due to the dehydroxylation of muscovite [20]. Three stages in the degradation curve of OM/P(2,3-DMA) can be observed, among which the initial two stages were the loss of water at 72°C and the degradation of organic compounds at 287°C . The final stage was the breaking of the polymer backbone (580°C) [21]. Along with degradation of P(2,3-DMA), muscovite also dissociates and results in the change of the surface structure. Therefore, it can be concluded that the decomposition proceeds with the formation of other products. The thermal stability of the composites obtained by TGA analysis is considerably better than that of pure P(2,3-DMA), because the

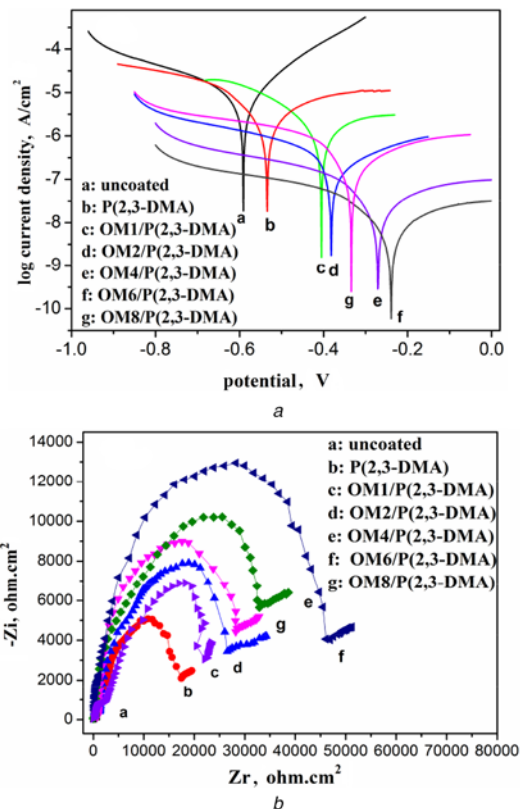


Fig. 6 Uncoated, P(2,3-DMA)-coated and OM/P(2,3-DMA)-coated (different clay concentrations) steel
a Tafel plots
b Nyquist plots

Table 1 Summary of literature with respect to the anticorrosion performance of the PCNs

Ref	Method	Clay/polymer	Metal	Electrolyte	E_{corr} , V
[1]	in situ emulsion polymerisation	polyaniline/MMT	Al	3.5 wt% NaCl	—
[5]	in situ intercalative polymerisation	poly(2,3-dimethylaniline)/kaolinite	steel	3.5 wt% NaCl	−0.274
[6]	in situ thermal polymerisation	polystyrene/MMT	steel	5 wt% NaCl	−0.329
[10]	in situ polymerisation	polystyrene/MMT	Al	3.5 wt% NaCl	−0.509
[11]	in situ chemical oxidative polymerisation	polyaniline/MMT	steel	1.0 M H ₂ SO ₄	−0.307
[17]	emulsion polymerisation	poly(o-methoxyaniline)/MMT	steel	5 wt% NaCl	−0.462
[18]	self-assembling and graft polymerisation	poly(2,3-dimethylaniline)/attapulgit	steel	3.5 wt% NaCl	—
[24]	emulsion polymerisation	poly(2,3-dimethylaniline)/MMT	Fe	3.5 wt% NaCl	−0.308

muscovite dispersion in P(2,3-DMA) provides a barrier to the diffusion of volatile compositions at elevated temperatures.

Fig. 5 depicts the SEM images of muscovite, P(2,3-DMA) and OM/P(2,3-DMA). The presence of platelets in muscovite was detected in SEM image Fig. 5a. Furthermore, Fig. 5b revealed that the agglomerated spheres exist in P(2,3-DMA). However, the size of the particles of muscovite decreased, and the agglomerated spheres could not be observed in OM/P(2,3-DMA) (Fig. 5c), demonstrating the possible intercalation and polymerisation of organic molecules between muscovite layers.

Fig. 6a shows the Tafel plots of the uncoated, P(2,3-DMA)-coated, and OM/P(2,3-DMA)-coated [i.e. 1, 2, 4, 6 and 8% (w/w) M] steel samples. The anticorrosion performance of the coating is positively correlated with the E_{corr} value and increases with an increase in the E_{corr} value [22]. Fig. 6a denotes that a series of OM/P(2,3-DMA) nanocomposite-coated steel electrodes exhibits higher E_{corr} values when compared with those of the pure P(2,3-DMA)-coated electrodes. Thus, the addition of muscovite can effectively increase the anticorrosion performance of pure polymers. At the low-level load of muscovite, the corrosion protection of the nanocomposites increases with an increase of the content of muscovite. However, the OM6/P(2,3-DMA) exhibits a higher corrosion resistance when compared with that of the OM8/P(2,3-DMA) nanocomposite. Thus, the optimal anticorrosive properties were obtained for the OM/P(2,3-DMA) coating with a 6 wt% OM. It is assumed that a small amount of muscovite can be better dispersed and stripped in the P(2,3-DMA) matrix and the P(2,3-DMA) molecular chain enters the interlayer of muscovite to form a composite structure. It can effectively block the spread of H₂O and O₂, and enhance the anticorrosion performance of the composite material. With a further increase in the content of muscovite, muscovite cannot be effectively dispersed. Thus, it peels off and easily agglomerates, which affected the P(2,3-DMA) polymerisation and decreased the anticorrosion performance of the composite [23].

The difference between the corrosion activities of the P(2,3-DMA)- and OM/P(2,3-DMA)-coated steels was characterised using electrochemical impedance spectroscopy. The larger the diameter of the semicircle (i.e. charge transfer resistance (R_{ct})), the lower the corrosion rate [19]. Fig. 6b shows the Nyquist plots of coatings of P(2,3-DMA), and the OM/P(2,3-DMA) with 1, 2, 4, 6 and 8 wt% OM. OM/P(2,3-DMA) has the best anticorrosion performance compared to that of P(2,3-DMA), and the OM8/P(2,3-DMA) coating provides more effective corrosion protection, which is consistent with the conclusions of potentiodynamic measurements (Fig. 6a). Table 1 presents the literature review with respect to the anticorrosion performance study of the PCN. From a survey of Table 1, the OM/P(2,3-DMA) prepared in this Letter is considered to be an efficient anticorrosive filler.

The major problem related to classical organic coatings is the penetration of corrosive agents (such as O₂ molecules) through the coating, as illustrated in Fig. 7a. When these agents reach the interface between the metal and coatings, the organic coatings degrade gradually and delaminate [25]. Fig. 7b presents a schematic

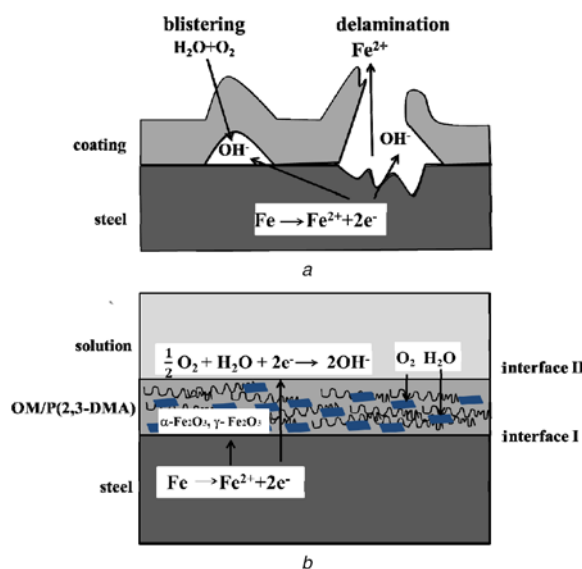
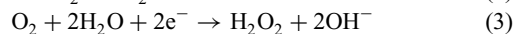
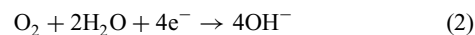


Fig. 7 Schematic representation of
a Corrosion of conventional coatings through delamination and blistering
b Proposed anticorrosion mechanisms of the OM/P(2,3-DMA) coatings on steel

illustrating the corrosion protection mechanism of OM/P(2,3-DMA) for steel. If P(2,3-DMA) is present in a coating and in contact with the electrolyte, the anodic dissolution of iron initially occurs through the pores in the coating.



P(2,3-DMA) withdraws charge from the metal, passivating its surfaces [26] and thus slowing the initial corrosion. However, P(2,3-DMA) may also serve as a centre or act similar to oligomers for oxygen reduction reactions (2) and (3)



These processes prevent the penetration of O₂ into the metal surface. Therefore, the P(2,3-DMA) acts as an active barrier [22, 25]. The OM can make the surface of the clay platelets straightforward to compatibilise within the polymer chains, thereby resulting in excellent dispersion in the polymer matrix, which could provide a higher tortuosity of diffusion path of corrosive agents [5]. In addition, the electrons generated by the anode are transferred from the metal surface (interface I) to the outside of the coating (interface II), owing to the electrical conductivity of P(2,3-DMA), and then react with O₂ to form OH[−]. Thus, there are no Fe²⁺ and OH[−] migration problems. Therefore, a dense oxide layer is

produced owing to the spatial separation of the cathodic and anodic partial reactions.

4. Conclusion: P(2,3-DMA), and PM/P(2,3-DMA) and OM/P(2,3-DMA) composites with exfoliated structures were successfully prepared via in situ chemical oxidation polymerisation process. The OM/P(2,3-DMA) coating considerably improved the anticorrosion performance of steel when compared with the P(2,3-DMA) coating because the muscovite plates were dispersed in the P(2,3-DMA) matrix, increasing the length of the diffusion path of H₂O and O₂ to the metal surface and hindering the diffusion of the corrosive agents.

5 References

- [1] Hosseini M.G., Jafari M., Najjar R.: 'Effect of polyaniline-montmorillonite nanocomposite powders addition on corrosion performance of epoxy coatings on Al 5000', *Surf. Coat. Technol.*, 2011, **206**, (2-3), pp. 280–286
- [2] Khalaf A.I., Assem Y., Yehia A.A.: 'Optical, dielectric, and mechanical properties of exfoliated poly(*N*, *N*-dimethylaminoethyl methacrylate)/clay nanocomposites prepared via In-situ bulk polymerization', *Polym. Compos.*, 2016, **39**, pp. 2603–2610
- [3] Mohaddespour A., Ahmadi S.J., Abolghasemi H.: 'The comparison of the behaviors of polymer/clay nanocomposites based on high density polyethylene and polypropylene in exposure of electron-irradiation', *Polym. Compos.*, 2009, **31**, (1), pp. 128–135
- [4] Hu H.F., Gan M.Y., Yan J., *ET AL.*: 'Enhancement of corrosion protection effect in poly(2,3-dimethylaniline) via the formation of nanofiber materials by introducing p-phenylenediamine', *Prog. Org. Coat.*, 2015, **81**, pp. 87–92
- [5] Yin H., Ma L., Gan M.Y., *ET AL.*: 'Preparation and properties of poly(2,3-dimethylaniline)/organic-kaolinite nanocomposites via in situ intercalative polymerization', *Compos. Sci. Technol.*, 2014, **94**, pp. 139–146
- [6] Yeh J.M., Liou S.J., Lin C.G., *ET AL.*: 'Effective enhancement of anticorrosive properties of polystyrene by polystyrene-clay nanocomposite materials', *J. Appl. Polym. Sci.*, 2004, **92**, (3), pp. 1970–1976
- [7] Maleki A., Kari T., Aghaei M.: 'Fe₃O₄@SiO₂/TiO₂-OSO₃H: an efficient hierarchical nanocatalyst for the organic quinazolines syntheses', *J. Porous Mater.*, 2017, **24**, (6), pp. 1481–1496
- [8] Ling Y., Long J.P.: 'Preparation and electrical conductivity of polythiophene/microcrystal muscovite layered composites', *Mater. Sci. Forum*, 2015, **814**, pp. 392–397
- [9] Maleki A., Hajizadeh Z., Firouzi-Haji R.: 'Eco-friendly functionalization of magnetic halloysite nanotube with SO₃H for synthesis of dihydropyrimidinones', *Microporous Mesoporous Mater.*, 2018, **259**, pp. 46–53
- [10] Maleki A.: 'Green oxidation protocol: selective conversions of alcohols and alkenes to aldehydes, ketones and epoxides by using a new multiwall carbon nanotube-based hybrid nanocatalyst via ultrasound irradiation', *Ultrason. Sonochem.*, 2018, **40**, pp. 460–464
- [11] Maleki A., Rahimi J.: 'Synthesis of dihydroquinazolinone and octahydroquinazolinone and benzimidazoloquinazolinone derivatives catalyzed by an efficient magnetically recoverable GO-based nanocomposite', *J. Porous Mater.*, 2018, **25**, pp. 1789–1796
- [12] Cheraghian G.: 'Synthesis and properties of polyacrylamide by nanoparticles, effect nanoclay on stability polyacrylamide solution', *Micro Nano Lett.*, 2017, **12**, (1), pp. 40–44
- [13] Najihah A.M.S., Zurina M., Ngadi N., *ET AL.*: 'The toughness, strength, and thermal properties enhancement of toughened polyamide 6 nanocomposite', 7th Brunei International Conference on Engineering and Technology 2018 (BICET 2018), Bandar Seri Begawan, Brunei, November 2018
- [14] Yeh J.M., Chang K.C.: 'Polymer/layered silicate nanocomposite anticorrosive coatings', *J. Ind. Eng. Chem.*, 2008, **14**, (3), pp. 275–291
- [15] Omar M.F., Akil H.M., Rasyid M.F.A., *ET AL.*: 'Thermal properties of polypropylene/muscovite layered silicate composites: effects of organic modifications and compatibilisers', *J. Compos. Mater.*, 2015, **49**, pp. 1195–1209
- [16] Omar M. F., Akil H.M., Ahmad Z.A., *ET AL.*: 'Effect of ion exchange treatment on dynamic compression properties of polypropylene/muscovite-layered silicate composites', *J. Thermoplast. Compos.*, 2016, **29**, (6), pp. 867–889
- [17] Gridi-Bennadji F., Beneu B., Laval J.P., *ET AL.*: 'Structural transformations of muscovite at high temperature by X-ray and neutron diffraction', *Appl. Clay Sci.*, 2008, **38**, (3-4), pp. 259–267
- [18] Yeh J.M., Chen C.L., Kuo T.H., *ET AL.*: 'Preparation and properties of (BATB-ODPA) polyimide-clay nanocomposite materials', *J. Appl. Polym. Sci.*, 2004, **92**, (2), pp. 1072–1079
- [19] Yeh J.M., Kuo T.H., Huang H.J., *ET AL.*: 'Preparation and characterization of poly(o-methoxyaniline)/Na⁺-MMT clay nanocomposite via emulsion polymerization: electrochemical studies of corrosion protection', *Eur. Polym. J.*, 2007, **43**, (5), pp. 1624–1634
- [20] Narayanan B.N., Koodathil R., Gangadharan T., *ET AL.*: 'Preparation and characterization of exfoliated polyaniline/montmorillonite nanocomposites', *Mater. Sci. Eng. B*, 2010, **168**, (1–3), pp. 242–244
- [21] Hu H.F., Gan M.Y., Ma L., *ET AL.*: 'Synthesis and anticorrosion property of poly(2,3-dimethylaniline)/organic-attapulgite nanofibers via self-assembling and graft polymerization', *Compos. Sci. Technol.*, 2014, **104**, pp. 9–17
- [22] Piromrueen P., Kongparakul S., Prasassarakich P.: 'Synthesis of polyaniline/montmorillonite nanocomposites with an enhanced anticorrosive performance', *Prog. Org. Coat.*, 2014, **77**, (3), pp. 691–700
- [23] Raju A., Lakshmi V., Vishnu Prataap R.K., *ET AL.*: 'Adduct modified nano-clay mineral dispersed polystyrene nanocomposites as advanced corrosion resistance coatings for aluminum alloys', *Appl. Clay Sci.*, 2016, **126**, pp. 81–88
- [24] Ma L., Fu D.D., Gan M.Y., *ET AL.*: 'Characterization and anticorrosive properties of poly(2,3-dimethylaniline)/Na⁺-montmorillonite composite prepared by emulsion polymerization', *J. Appl. Polym. Sci.*, 2013, **130**, pp. 4528–4533
- [25] Grgur B.N., Elkais A.R., Gvozdenović M.M., *ET AL.*: 'Corrosion of mild steel with composite polyaniline coatings using different formulations', *Prog. Org. Coat.*, 2015, **79**, pp. 17–24
- [26] Fahlman M., Jasty S., Epstein A.J.: 'Corrosion protection of iron/steel by emeraldine base polyaniline: an X-ray photoelectron spectroscopy study', *Synth. Met.*, 1997, **85**, pp. 1323–1326